Science

MAAAS

**Evidence for Upwelling of Corrosive "Acidified"
Water onto the Continental Shelf**

Richard A. Feely, *et al.*
Science **320**, 1490 (2008);
DOI: 10.1126/science.1155676

Evidence for Upwelling of Corrosive "Acidified" Water onto the Continental Shelf

Richard A. Feely,[1]* Christopher L. Sabine,[1] J. Martin Hernandez-Ayon,[2] Debby Ianson,[3] Burke Hales[4]

The absorption of atmospheric carbon dioxide (CO_2) into the ocean lowers the pH of the waters. This so-called ocean acidification could have important consequences for marine ecosystems. To better understand the extent of this ocean acidification in coastal waters, we conducted hydrographic surveys along the continental shelf of western North America from central Canada to northern Mexico. We observed seawater that is undersaturated with respect to aragonite upwelling onto large portions of the continental shelf, reaching depths of ~40 to 120 meters along most transect lines and all the way to the surface on one transect off northern California. Although seasonal upwelling of the undersaturated waters onto the shelf is a natural phenomenon in this region, the ocean uptake of anthropogenic CO_2 has increased the areal extent of the affected area.

Over the past 250 years, the release of carbon dioxide (CO_2) from industrial and agricultural activities has resulted in atmospheric CO_2 concentrations that have increased by about 100 parts per million (ppm). The atmospheric concentration of CO_2 is now higher than it has been for at least the past 650,000 years, and is expected to continue to rise at an increasing rate, leading to pronounced changes in our climate by the end of this century (1). Since the beginning of the industrial era, the oceans have absorbed ~127 ± 18 billion metric tons of carbon as CO_2 from the atmosphere, or about one-third of the anthropogenic carbon emissions released (2). This process of absorption of anthropogenic CO_2 has benefited humankind by substantially reducing the greenhouse gas concentrations in the atmosphere and minimizing some of the impacts of global warming. However, the ocean's daily uptake of 22 million metric tons of CO_2 has a sizable impact on its chemistry and biology. Recent hydrographic surveys and modeling studies have confirmed that the uptake of anthropogenic CO_2 by the oceans has resulted in a lowering of seawater pH by about 0.1 since the beginning of the industrial revolution (3–7). In the coming decades, this phenomenon, called "ocean acidification," could affect some of the most fundamental biological and geochemical processes of the sea and seriously alter the fundamental structure of pelagic and benthic ecosystems (8).

Estimates of future atmospheric and oceanic CO_2 concentrations, based on the Intergovernmental Panel on Climate Change (IPCC) CO_2 emission scenarios and general circulation models, indicate that atmospheric CO_2 concentrations could exceed 500 ppm by the middle of this century, and 800 ppm near the end of the century. This increase would result in a decrease in surface-water pH of ~0.4 by the end of the century, and a corresponding 50% decrease in carbonate ion concentration (5, 9). Such rapid changes are likely to negatively affect marine ecosystems, seriously jeopardizing the multifaceted economies that currently depend on them (10).

The reaction of CO_2 with seawater reduces the availability of carbonate ions that are necessary for calcium carbonate ($CaCO_3$) skeleton and shell formation for marine organisms such as corals, marine plankton, and shellfish. The extent to which the organisms are affected depends largely on the $CaCO_3$ saturation state (Ω), which is the product of the concentrations of Ca^{2+} and CO_3^{2-} divided by the apparent stoichiometric solubility product for either aragonite or calcite:

$$\Omega_{arag} = [Ca^{2+}][CO_3^{2-}]/K'_{sp_{arag}} \qquad (1)$$

$$\Omega_{cal} = [Ca^{2+}][CO_3^{2-}]/K'_{sp_{cal}} \qquad (2)$$

where the calcium concentration is estimated from the salinity, and the carbonate ion con-

[1]Pacific Marine Environmental Laboratory/National Oceanic and Atmospheric Administration, 7600 Sand Point Way NE, Seattle, WA 98115–6349, USA. [2]Instituto de Investigaciones Oceanologicas, Universidad Autonoma de Baja California, Km. 103 Carr. Tijuana-Ensenada, Ensenada, Baja California, Mexico. [3]Fisheries and Oceans Canada, Institute of Ocean Science, Post Office Box 6000, Sidney, BC V8L 4B2, Canada. [4]College of Oceanic and Atmospheric Sciences, Oregon State University, 104 Ocean Administration Building, Corvallis, OR 97331–5503, USA.

*To whom correspondence should be addressed. E-mail: richard.a.feely@noaa.gov
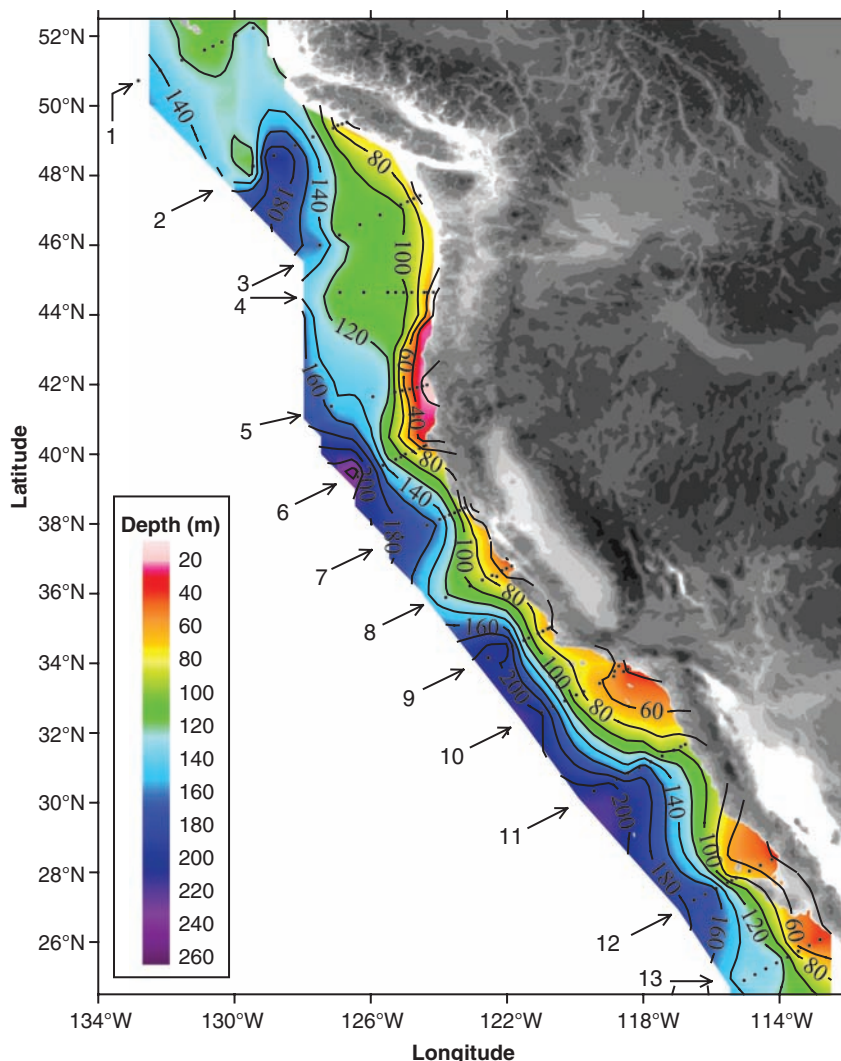

Fig. 1. Distribution of the depths of the undersaturated water (aragonite saturation < 1.0; pH < 7.75) on the continental shelf of western North America from Queen Charlotte Sound, Canada, to San Gregorio Baja California Sur, Mexico. On transect line 5, the corrosive water reaches all the way to the surface in the inshore waters near the coast. The black dots represent station locations.

centration is calculated from the dissolved inorganic carbon (DIC) and total alkalinity (TA) measurements (*11*). In regions where Ω_{arag} or Ω_{cal} is > 1.0, the formation of shells and skeletons is favored. Below a value of 1.0, the water is corrosive and dissolution of pure aragonite and unprotected aragonite shells will begin to occur (*12*). Recent studies have shown that in many regions of the ocean, the aragonite saturation horizon shoaled as much as 40 to 200 m as a direct consequence of the uptake of anthropogenic CO_2 (*3*, *5*, *6*). It is shallowest in the northeastern Pacific Ocean, only 100 to 300 m from the ocean surface, allowing for the transport of undersaturated waters onto the continental shelf during periods of upwelling.

In May and June 2007, we conducted the North American Carbon Program (NACP) West Coast Cruise on the Research Ship *Wecoma* along the continental shelf of western North America, completing a series of 13 cross-shelf transects from Queen Charlotte Sound, Canada, to San Gregorio Baja California Sur, Mexico (Fig. 1). Full water column conductivity-temperature-depth rosette stations were occupied at specified locations along each transect (Fig. 1). Water samples were collected in modified Niskin-type bottles and analyzed for DIC, TA, oxygen, nutrients, and dissolved and particulate organic carbon. Aragonite and calcite saturation, seawater pH (pH$_{SW}$), and partial pressure of CO_2 (pCO$_2$) were calculated from the DIC and TA data (*11*).

The central and southern coastal region off western North America is strongly influenced by seasonal upwelling, which typically begins in early spring when the Aleutian low-pressure system moves to the northwest and the Pacific High moves northward, resulting in a strengthening of the northwesterly winds (*13*, *14*). These winds drive net surface-water Ekman transport offshore, which induces the upwelling of CO_2-rich, intermediate-depth (100 to 200 m) offshore waters onto the continental shelf. The upwelling lasts until late summer or fall, when winter storms return.

During the cruise, various stages and strengths of upwelling were observed from line 2 off central Vancouver Island to line 11 off Baja California, Mexico. We observed recent upwelling on lines 5 and 6 near the Oregon-California border. Coincident with the upwelled waters, we found evidence for undersaturated, low-pH seawater in the bottom waters as depicted by Ω_{arag} values < 1.0 and pH values < 7.75. The corrosive waters reached mid-shelf depths of ~40 to 120 m along lines 2 to 4 and lines 7 to 13 (Fig. 1). In the region of the strongest upwelling (line 5), the isolines of Ω_{arag} = 1.0, DIC = 2190, and pH = 7.75 closely followed the 26.2 potential density surface (Fig. 2). This density surface shoaled from a depth of ~150 m in the offshore waters and breached the surface over the shelf near the 100-m bottom contour, ~40 km from the coast. This shoaling of the density surfaces and CO_2-rich waters as one approaches land is typical of strong coastal upwelling conditions (*15–18*). The surface-water pCO$_2$ on the 26.2 potential density surface was about 850 µatm near the shelfbreak and higher inshore (Fig. 2), possibly enhanced by respiration processes on the shelf (*17*). These results indicate that the upwelling process caused the entire water column shoreward of the 50-m bottom contour to become undersaturated with respect to aragonite, a condition that was not predicted to occur in open-ocean surface waters until 2050 (*5*). On line 6, the next transect south, the undersaturated water was close to the surface at ~22 km from the coast. The lowest Ω_{arag} values (<0.60) observed in the near-bottom waters of the continental shelf corresponded with pH values close to 7.6. Because the calcite saturation horizon is located between 225 and 400 m in this part of the northeastern Pacific (*19*), it is still too deep to shoal onto the continental shelf. Nevertheless, the calcite saturations values drop in the core of the upwelled water (Ω_{cal} < 1.3).

As noted, the North Pacific aragonite saturation horizons are among the shallowest in the global ocean (*3*). The uptake of anthropogenic CO_2 has caused these horizons to shoal by 50 to 100 m since preindustrial times so that they are within the density layers that are currently being upwelled along the west coast of North America.
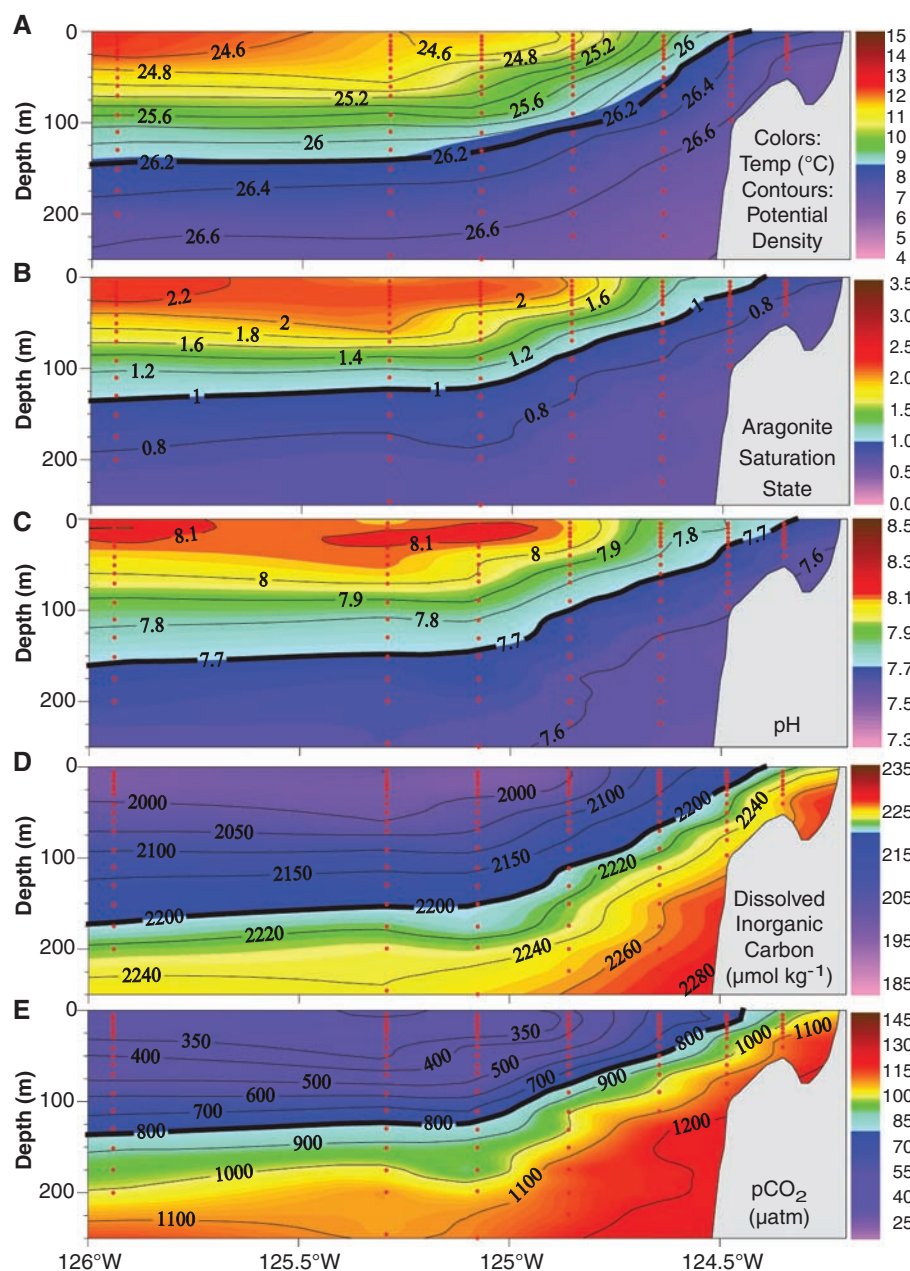

Fig. 2. Vertical sections of (**A**) temperature, (**B**) aragonite saturation, (**C**) pH, (**D**) DIC, and (**E**) pCO$_2$ on transect line 5 off Pt. St. George, California. The potential density surfaces are superimposed on the temperature section. The 26.2 potential density surface delineates the location of the first instance in which the undersaturated water is upwelled from depths of 150 to 200 m onto the shelf and outcropping at the surface near the coast. The red dots represent sample locations.

Although much of the corrosive character of these waters is the natural result of respiration processes at intermediate depths below the euphotic zone, this region continues to accumulate more anthropogenic CO_2 and, therefore, the upwelling processes will expose coastal organisms living in the water column or at the sea floor to less saturated waters, exacerbating the biological impacts of ocean acidification.

On the basis of our observed O_2 values and estimated O_2 consumption rates on the same density surfaces ([18–20]), the upwelled water off northern California (line 5) was last at the surface about 50 years ago, when atmospheric CO_2 was about 65 ppm lower than it is today. The open-ocean anthropogenic CO_2 distributions in the Pacific have been estimated previously ([4, 19, 21]). By determining the density dependence of anthropogenic CO_2 distributions in the eastern-most North Pacific stations of the Sabine et al. ([21]) data set, we estimate that these upwelled waters contain ~$31 \pm 4 \,\mu mol \, kg^{-1}$ anthropogenic CO_2 (fig. S2). Removing this signal from the DIC increases the aragonite saturation state of the waters by about 0.2 units. Thus, without the anthropogenic signal, the equilibrium aragonite saturation level ($\Omega_{arag} = 1$) would be deeper by about 50 m across the shelf, and no undersaturated waters would reach the surface. Water already in transit to upwelling centers carries increasing anthropogenic CO_2 and more corrosive conditions to the coastal oceans of the future. Thus, the undersaturated waters, which were mostly a problem for benthic communities in the deeper waters near the shelf break in the preindustrial era, have shoaled closer to the surface and near the coast because of the additional inputs of anthropogenic CO_2.

These observations clearly show that seasonal upwelling processes enhance the advancement of the corrosive deep water into broad regions of the North American western continental shelf. Because the region experiences seasonal periods of enhanced aragonite undersaturation, it is important to understand how the indigenous organisms deal with this exposure and whether future increases in the range and intensity of the corrosiveness will affect their survivorship. Presently, little is known about how this intermittent exposure to corrosive water might affect the development of larval, juvenile, and adult stages of aragonitic calcifying organisms or finfish that populate the neritic and benthic environments in this region and fuel a thriving economy. Laboratory and mesocosm experiments show that these changes in saturation state may cause substantial changes in overall calcification rates for many species of marine calcifiers including corals, coccolithophores, foraminifera, and pteropods, which are a major food source for local juvenile salmon ([8, 22–30]). Similar decreases in calcification rates would be expected for edible mussels, clams, and oysters ([22, 31]). Other research indicates that many species of juvenile fish and shellfish of economic importance to coastal regions are highly sensitive to higher-than-normal CO_2 concentrations such that high rates of mortality are directly correlated with the higher CO_2 concentrations ([31, 32]). Although comprehensive field studies of organisms and their response to sporadic increases in CO_2 along the western North American coast are lacking, current studies suggest that further research under field conditions is warranted. Our results show that a large section of the North American continental shelf is affected by ocean acidification. Other continental shelf regions may also be affected where anthropogenic CO_2-enriched water is being upwelled onto the shelf.

References and Notes
1. U. Siegenthaler et al., Science **310**, 1313 (2005).
2. C. L. Sabine, R. A. Feely, in Greenhouse Gas Sinks, D. Reay, N. Hewitt, J. Grace, K. Smith, Eds. (CABI, Oxfordshire, UK, 2007).
3. R. A. Feely et al., Science **305**, 362 (2004).
4. C. L. Sabine et al., Science **305**, 367 (2004).
5. J. C. Orr et al., Nature **437**, 681 (2005).
6. K. Caldeira, M. E. Wickett, J. Geophys. Res. Oceans **110**, 365 (2005).
7. R. A. Feely et al., PICES Press **16**, 22 (2008).
8. J. A. Kleypas et al., "Impacts of Increasing Ocean Acidification on Coral Reefs and Other Marine Calcifiers: A Guide for Future Research," report of a workshop held 18 to 20 April 2005, St. Petersburg, FL, sponsored by NSF, NOAA, and the U.S. Geological Survey (2006).
9. S. Solomon et al., Eds, in Contribution of Working Group I to the Fourth Assessment Report of the Intergovernmental Panel on Climate Change (Cambridge Univ. Press, Cambridge and New York, 2007).
10. J. Raven et al., "Ocean acidification due to increasing atmospheric carbon dioxide," policy document 12/05 (The Royal Society, London, 2005).
11. The details of the analytical methods and calculations for the carbonate system and anthropogenic CO_2 are given in the supporting online material.
12. R. A. Feely et al., Mar. Chem. **25**, 227 (1988).
13. B. Hickey, in The Sea, A. R. Robinson, K. H. Brink, Eds. (Wiley, New York, 1998), vol. 2.
14. J. Timothy Pennington, F. P. Chavez, Deep Sea Res. Part II Top. Stud. Oceanogr. **47**, 947 (2000).
15. A. van Geen et al., Deep Sea Res. Part II Top. Stud. Oceanogr. **47**, 975 (2000).
16. G. E. Friederich, P. M. Walz, M. G. Burczynski, F. P. Chavez, Prog. Oceanogr. **54**, 185 (2002).
17. D. Ianson et al., Deep Sea Res. Part I Oceanogr. Res. Pap. **50**, 1023 (2003).
18. B. Hales et al., Global Biogeochem. Cycles **19**, 10.1029/2004GB002295 (2005).
19. R. A. Feely et al., Global Biogeochem. Cycles **16**, 1144 (2002).
20. R. A. Feely et al., J. Oceanogr. **60**, 45 (2004).
21. C. L. Sabine et al., Global Biogeochem. Cycles **16**, 1083 (2002).
22. M. A. Green, M. E. Jones, C. L. Boudreau, R. L. Moore, B. A. Westman, Limnol. Oceanogr. **49**, 727 (2004).
23. J. M. Guinotte et al., Coral Reefs **22**, 551 (2003).
24. C. Langdon, M. J. Atkinson, J. Geophys. Res. Oceans **110**, C09S07 (2005).
25. H. J. Spero et al., Nature **390**, 497 (1997).
26. U. Riebesell et al., Nature **407**, 364 (2000).
27. I. Zondervan et al., Global Biogeochem. Cycles **15**, 507 (2001).
28. B. A. Seibel, V. J. Fabry, Adv. Appl. Biodivers. Sci. **4**, 59 (2003).
29. B. Delille et al., Global Biogeochem. Cycles **19**, GB2023 (2005).
30. A. Engel et al., Limnol. Oceanogr. **50**, 493 (2005).
31. F. Gazeau et al., Geophys. Res. Lett. **34**, L07603 (2007).
32. A. Ishimatsu et al., J. Oceanogr. **60**, 731 (2004).
33. We thank Captain Richard Verlini and the crew of the R/V Wecoma for logistics support. We also thank D. Greeley, D. Wisegarver, P. Covert, and S. Barry for the DIC and TA measurements. Financial support for this work was provided by the National Oceanic and Atmospheric Administration's Global Carbon Cycle Program and the National Aeronautical and Space Administration Ocean Biology and Biogeochemistry Program.

Regulation of Hepatic Lipogenesis by the Transcription Factor XBP1

Ann-Hwee Lee,[1]* Erez F. Scapa,[2,3] David E. Cohen,[2,3] Laurie H. Glimcher[1,2]*

Dietary carbohydrates regulate hepatic lipogenesis by controlling the expression of critical enzymes in glycolytic and lipogenic pathways. We found that the transcription factor XBP1, a key regulator of the unfolded protein response, is required for the unrelated function of normal fatty acid synthesis in the liver. XBP1 protein expression in mice was elevated after feeding carbohydrates and corresponded with the induction of critical genes involved in fatty acid synthesis. Inducible, selective deletion of XBP1 in the liver resulted in marked hypocholesterolemia and hypotriglyceridemia, secondary to a decreased production of lipids from the liver. This phenotype was not accompanied by hepatic steatosis or compromise in protein secretory function. The identification of XBP1 as a regulator of lipogenesis has important implications for human dyslipidemias.

Hepatic lipid synthesis increases upon ingestion of excess carbohydrates, which are converted into triglyceride (TG) in the liver and transported to adipose tissue for energy storage. Dysregulation of hepatic lipid metabolism is closely related to the development of metabolic syndrome, a condition characterized by central obesity, dyslipidemia, elevated blood glucose, and hypertension ([1]). In mammals, hepatic lipid metabolism is controlled by transcription factors, such as liver X receptor (LXR), sterol regulatory element–binding proteins (SREBPs), and carbohydrate response element–binding protein (ChREBP), that regulate the expression of

[1]Department of Immunology and Infectious Diseases, Harvard School of Public Health, Boston, MA 02115, USA. [2]Department of Medicine, Harvard Medical School, Boston, MA 02115, USA. [3]Division of Gastroenterology, Brigham and Women's Hospital, Boston, MA 02115, USA.

*To whom correspondence should be addressed. E-mail: lglimcher@hsph.harvard.edu (L.H.G.); ahlee@hsph.harvard.edu (A.-H.L.)

Supporting Online Material for

Evidence for Upwelling of Corrosive "Acidified" Water onto the Continental Shelf

Richard A. Feely,[*] Christopher L. Sabine, J. Martin Hernandez-Ayon, Debby Ianson, Burke Hales

*To whom correspondence should be addressed. E-mail: richard.a.feely@noaa.gov

This PDF file includes:

Materials and Methods
Figs. S1 and S2
References

Correction: The originally posted supporting online material contained a misstatement about the quality assurance procedure for assessing the alkalinity data. The fifth sentence of the second paragraph should read: The replicate samples were interspersed throughout the station analysis for quality assurance.

Science Supporting Online Material

Evidence for Upwelling of Corrosive 'Acidified' Water onto the Continental Shelf

Richard A. Feely, Christopher L. Sabine, J. Martin Hernandez-Ayon, Debby Ianson, and Burke Hales

Sampling and Analytical Methods

For the NACP West Coast Cruise, samples were collected and analyzed for dissolved

inorganic carbon (DIC), total alkalinity (TA), and hydrographic data along 13 cross-shelf

transects from Queen Charlotte Sound, Canada to San Gregorio Baja California Sur,

Mexico. Dissolved inorganic carbon (DIC) and total alkalinity (TA) were measured on all

the samples and pH_{SW} (pH is reported using the seawater scale) and pCO_2 were

calculated from the resulting data utilizing the program of Lewis and Wallace (*S1*).

Samples were drawn from the Niskin-type bottles into cleaned, precombusted 300-mL

Pyrex bottles using Tygon tubing with silicone ends. DIC was determined by gas

extraction and coulometry using a modified Single-Operator Multi-Metabolic Analyzer

(SOMMA) system (*S2-S5*). The precision for DIC was ± 1.5 μmol kg^{-1}.

Seawater TA was measured by acidimetric titration, employing the open cell method

described by Dickson et al (*S6, S7*). This method involves first acidifying the sample to

reduce the sample pH to less than 3.6 followed by bubbling CO_2-free air through the

sample to facilitate removal of the CO_2 evolved by the acid addition. After removal of

the carbonate species from solution, the titration proceeds until a pH of less than 3.0 is

attained. The precision for TA was ± 2.0 μmol kg^{-1}. Replicate samples were typically

taken from the two samples out of each station. The replicate samples were interspersed

throughout the station analysis for quality assurance. No systematic differences between the replicates were observed. The data quality was confirmed by daily analyses of Certified Reference Materials (*S8*).

Aragonite and calcite saturation levels were calculated using the program developed by Lewis and Wallace (*S1*) that included the carbonic acid dissociation constants of Merhbach (*S9*) as refit by Dickson and Millero (*S10*). The *in-situ* degree of saturation of seawater with respect to aragonite and calcite is the ion product of the concentrations of calcium and carbonate ions, at the in situ temperature, salinity and pressure, divided by the apparent stoichiometric solubility product for those conditions, where the Ca^{+2} concentrations are estimated from the salinity and the carbonate ion concentration is calculated from the DIC and total alkalinity TA data. The pressure affect on the solubility is estimated from the equation of Mucci (*S11*) that includes the adjustments to the constants recommended by Millero (*S12*).

Anthropogenic CO_2 in the Northeastern Pacific

The anthropogenic CO_2 of the coastal waters was determined one of two ways. The higher density waters ($\sigma_\theta > 25.0$) were presumed to be consistent with open ocean waters. The large-scale open ocean anthropogenic CO_2 distributions were evaluated by Sabine et al. (*S13*) for the entire Pacific using the ΔC^* method. These estimates require a water mass age tracer, such as chlorofluorocarbons, which were not available for the coastal waters. Therefore, we took a subset of the stations used by Sabine et al. (*S13*) that were between 21 - 60°N and 140-109°W (Fig. *S1*) and fit the estimated anthropogenic CO_2 concentrations as a function of potential density (Fig. *S2*).

Anthropogenic $CO_2 = -2742 + 225.31\ (\sigma_\theta) - 4.5604\ (\sigma_\theta)^2$ (*S1*)

The data were limited to the upper 250 m of the water column since that is the maximum depth of the coastal sections presented here. The anthropogenic CO_2 of the coastal waters was then calculated from potential density using equation *S1*. The highest densities were comparable between the open ocean and the coastal waters.

The lower density waters (σ_θ<25.0) are generally found very near the surface or represent coastal waters with river influences. Either way, these waters are not as strongly connected with the subsurface open-ocean waters and are much more likely to be tracking the current atmospheric CO_2 concentrations. To estimate the pre-industrial DIC concentration of these waters, the measured DIC and TA were used to calculate pCO_2. The calculated pCO_2 was then decreased by the change in atmospheric CO_2 between 1800 and 2007. This revised pCO_2 was then used together with the TA to calculate a pre-industrial DIC. The difference between the measured DIC and the estimated pre-industrial DIC is taken as the anthropogenic CO_2 of these waters. This is the same approach used by Sabine et al. (*S13*) and others for determining surface water anthropogenic CO_2 concentrations.
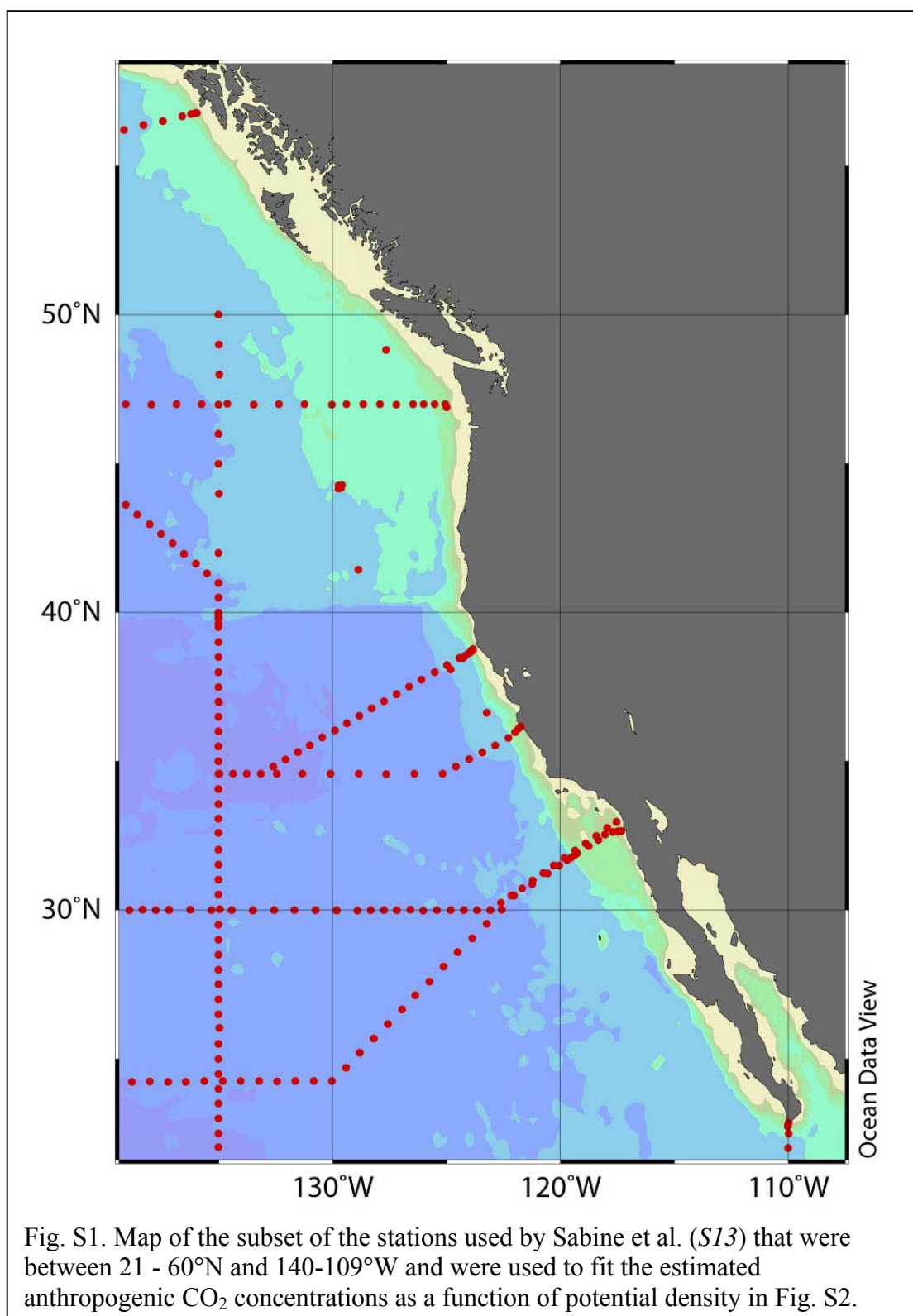
The boundary between these two methods was chosen to be σ_θ=25.0 because the potential density versus anthropogenic CO_2 function showed much larger scatter at σ_θ<25.0 Also, a σ_θ of 25.0 represents the highest density of surface waters from the open-ocean data set, thus cutting all waters with densities lighter than 25.0 eliminated the variable surface waters from the fit.

There are many sources of uncertainty with these crude calculations. The open-ocean ΔC^* calculations for this region yields a calculated RMS error for anthropogenic CO_2 of $\pm$ 4 μmol kg^{-1}. There are many other sources of uncertainty here including the quality of

the density versus anthropogenic CO_2 fit, the similarity between coastal and open ocean waters, and the temporal stability of parameters such as the total alkalinity in the coastal region. On the other hand, it is not likely that there is zero anthropogenic CO_2 in the coastal waters and it is not likely that the anthropogenic CO_2 has increased significantly faster than the growth rate of CO_2 in the atmosphere. Based on these considerations, we believe that these estimates are good to within $\pm$ 50%.

References and Notes

S1. E. Lewis and D. W. R. Wallace, Program developed for CO_2 system calculations, Report 105, Oak Ridge National Laboratory, 33 pp. (Also available currently at: http://cdiac.esd.ornl.gov/oceans/co2rprt.html). (1998).

S2. K. M. Johnson *et al., Marine Chemistry (16)*, 61-82 (1985).

S3. K. M. Johnson *et al., Marine Chemistry, 21(2)*, 117-133 (1987).

S4. K. M. Johnson and D.W.R. Wallace. DOE Research Summary No. 19, Carbon Dioxide Information Analysis Center, Oak Ridge National Laboratory (1992).

S5. DOE Handbook of methods for the analysis of the various parameters of the carbon dioxide system in sea water. Version 2, A.G. Dickson and C. Goyet, eds., ORNL/CDIAC-74. (1994).

S6. A. G. Dickson *Oceanography, 14(4),* 21-22. (2001).

S7. A.G. Dickson *et al., Guide to Best Practices for Ocean CO_2 Measurements,* PICES Special Publication No. 3, 191 pp.

S8. A. G. Dickson *et al., Marine Chemistry, 80,* 185-197 (2003).

S9. C. Mehrbach *et al., Limnol. Oceanogr., 18*, 897–907. (1973).

S10. A. G. Dickson and F. J. Millero *Deep-Sea Res., 34*, 1733–1743. (1987).

S11. A. Mucci **Am. J. Sci., 238,** 780–799, 1983.

S12. F. J. Millero *Geochim. Cosmochim. Acta, 59(4),* 661–677. (1995).

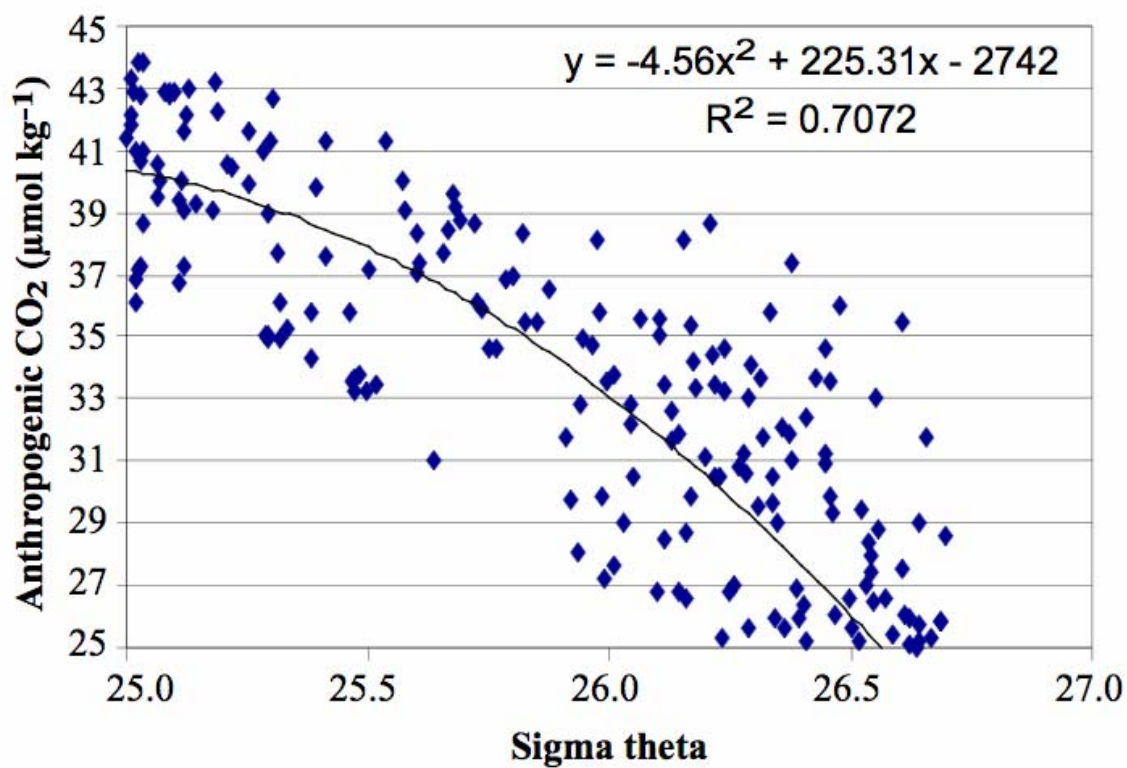S13. C. L. Sabine *et al., Global Biogeochem. Cycles, 16*(4), 1083, doi: 10.1029/2001GB001639. (2002).

Fig. S1. Map of the subset of the stations used by Sabine et al. (*S13*) that were between 21 - 60°N and 140-109°W and were used to fit the estimated anthropogenic CO_2 concentrations as a function of potential density in Fig. S2.

5

Fig. S2. Plot of the distribution of anthropogenic CO_2 in $\mu mol\ kg^{-1}$ as a function of potential density for stations from the northeastern Pacific as shown in Fig. S1 above.